ACS OMEGA

Open Access

http://pubs.acs.org/journal/acsodf

Article

Self-Reinforced Biocomposites Made from Poly(3-hydroxybutyrate-*co*-3-hydroxyvalerate) (PHBV): An Innovative Approach to Sustainable Packaging Production through Melt Processing

Anja Schmidt,* Birgit Bittmann-Hennes, Danny Moncada, and Belén Montero

Cite This: *ACS Omega* 2024, 9, 51073−51088

Read Online

ACCESS | Metrics & More | Article Recommendations | Supporting Information

ABSTRACT: The production of self-reinforced composites allows for a targeted tailoring of the property profile for specific applications and offers the physical-mechanical advantages of a synergistic combination of the two components with a high value in terms of their end-of-life scenarios. This study deals with the preparation and evaluation of self-reinforced biocomposites of poly(3-hydroxybutyrate-*co*-3-hydroxyvalerate) (PHBV) with PHBV microparticles produced for the first time by industry-oriented melt processing. First, microparticles with a size of 4 μm were prepared and characterized by using the miniemulsion/evaporation technique. These microparticles were then incorporated into the PHBV matrix by extrusion and injection molding. Electron microscopy revealed particles in biocomposites. The results indicate heterogeneous nucleation, leading to higher crystallinity at higher melting temperatures. This leads to a slight embrittlement and an improvement of the barrier properties against oxygen and water vapor. These industrially produced biocomposites benefit from particles by showing, among other things, higher barrier properties while retaining their green character, making them promising and easily accessible candidates for future packaging applications.

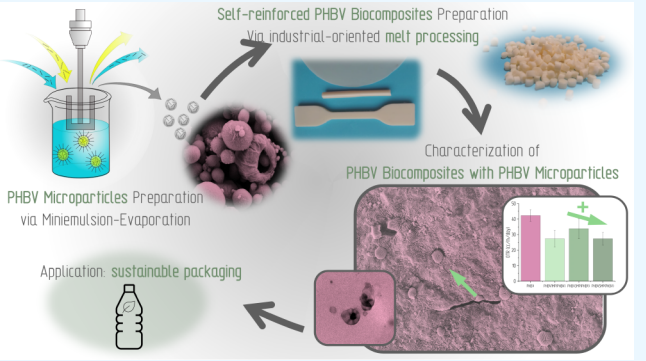

INTRODUCTION

More than millions of plastic pellets were swept onto the northwest coast of Europe in spring 2024 due to a tanker accident. This gives reason to the EU to rethink the guidelines for handling plastic in order to further strengthen sustainable use.[1] The packaging industry accounts for a large proportion of the global plastic production. However, especially widely used multilayer packaging is challenging to recycle, and the separation of the layers is both energy-intensive and costly.[2] Here, bioplastics and their composites are playing an increasingly important role, as they can comply with the new regulations thanks to recent research on improved handling and production.

With a predicted production volume of 133 million tons worldwide in 2024, polyhydroxyalkanoates (PHAs) are one of the most promising biobased and biodegradable biopolymers.[3] They are a group of biobased polyesters that are formed by a variety of microorganisms as carbon and energy stores and can contribute to their stress robustness.[4,5] The high price of PHAs is still hindering their widespread commercial use. It currently costs on average around five times more than comparable commercially available plastics.[6] This is mainly due to the high production costs, with the feedstock accounting for almost 45%.[7] It is therefore crucial for the future to make production more cost-efficient. The industry is currently focused on microbial fermentation, which determines the yield and quality of PHAs through the choice of microbial strain, carbon source, fermentation apparatus, agitation parameters, recovery method, and secondary crystallization factors.[8] In order to improve competitiveness, further developments that lead to higher productivity and quality are therefore crucial. In addition to more specialized bacterial strains for fermentation, these include the use of waste streams as raw materials or the introduction of new technologies. This includes, for example, the use of genetically modified bacterial strains to increase yields, obtain cheaper raw material, or improve recovery. Cyanobacteria that enable the utilization of CO_2 as a carbon source or extremophiles that can be used in next-generation industrial biotechnologies (NGIBs) are also currently part of the research.[3,7,9−15]

Polyhydroxyalkanoates are a group of biobased isotactic polyesters. They are commonly composed of *R*-hydroxy fatty acids, each monomer of which contains a saturated alkyl group

Received: June 27, 2024
Revised: November 1, 2024
Accepted: November 26, 2024
Published: December 17, 2024

with side chains consisting of unsaturated or branched alkyl groups.[16] The material properties are mainly determined by the length of the polymer chains, as well as the type and distribution of the monomer blocks. More than 150 different hydroxyalkanoic acid (HA) building blocks have been found.[17] The simplest polyester in this group is poly(3-hydroxybutyrate) (P3HB) with a methyl group as a side group. This allows a very high crystallinity, which results in high brittleness and high melting temperatures but relatively low decomposition temperatures resulting in a limited process range. Copolymerization with hydroxy valerate, respectively, an ethyl group, helps to overcome these disadvantages.[18] In general, poly(3-hydroxybutyrate-*co*-3-hydroxyvalerate) (PHBV) exhibits lower crystallinity, which results in lower melting temperatures[19] and a broadening of the process window; it also has a positive effect on flexibility.[20] The proportion of 3HV has a significant influence on properties. The higher is the 3HV content, the lower is the growth rate of the spherulites, the lower are the melting temperatures,[21,22] the lower is the crystallinity, and the smaller are the spherulites[23] and the higher is the ductility with better strength and toughness. The mechanical properties are comparable to those of conventional polymers such as polypropylene (PP) or polyethylene (PE).[8] The sensitivity of the polymer chains to thermomechanical degradation is the challenge for the melt processing of these polymers.[24−28] To prevent chain degradation, it is crucial to define adequate manufacturing parameters. Plasticizers are used to reduce melting temperatures and viscosity to prevent degradation.[29,30] In addition to thermal degradation,[25] PHBV is also characterized by biodegradability in many anaerobic and aerobic environments across different media.[31,32] Moreover, it is nontoxic and has good biocompatibility with many cells.[20,33] PHBV is also characterized by very good barrier properties, which are on a par with good commercial polymers such as polyvinylchloride (PVC) and polyethylene terephthalate (PET).[34,35]

Due to their diverse properties and versatile processing options, PHAs are used in many areas, for example, in the textile sector (spun fibers), in cosmetic products, in medical applications (drug delivery, tissue scaffolds, membrane implants, bone tissue engineering, cardiac implants, vascular grafts, artificial nerve conduits, drug delivery matrices, and nutritional and therapeutic applications), in agricultural technology (mulch films, agricultural nets, and agricultural grow bags) and others such as denitrification.[36−41] One of the main applications of PHBV is the packaging industry.[42] Different types of packaging can be produced by using a wide range of industrial manufacturing methods. Melt processing, such as extrusion and injection, is already widely used to produce films and rigid packaging. Electrospinning of fibers, additive manufacturing of components, or coating strategies are also explored.[30,43−47]

In order to be able to adapt the properties more specifically to the requirements, PHAs are often used as blends with other polymers or as biocomposites with different fillers such as fibers or particles.[48,49] These are, for example, nanofillers, natural fibers, agricultural waste, clay, silicate, cellulose materials, microparticles, etc.[42,50,51] Furthermore, the incorporation of active substances such as antimicrobial, antioxidant, or regenerative agents is being investigated in order to adapt the functional performance.[52,53] However, the incorporation of fillers from other material classes often creates an end-of-life problem, as recyclability is almost impossible, and depending on the filler, the biodegradability of the complete material system is no longer guaranteed.

Self-reinforced composites (SRCs), self-reinforced polymers (SRPs), or single polymers provide an advantage in this respect, as they have a high value as a recycle product due to their homogeneity. Thanks to their pure chemical functionality and excellent interface between the components, they offer outstanding properties for many applications.[54] Furthermore, for PHBVs, this means preserving their green character and the possibility of biodegradability/composting as an alternative for the end of life.[55] In the literature, SRCs are often used for multilayered, fiber, or particle technologies.[56,57] For example, Wang et al.[58] incorporate PP fiber into PP film, and Zherebtsov et al.[56] incorporate ultra-high molecular weight polyethylene (UHMWPE) fibers in an isotropic UHMWPE layer. Yadav et al.[57] and Le Gall[59] investigate (stereocomplex or bicomponent) PLA fibers in PLA matrices for filament fabrication, and they show a significant increase in mechanical properties. In contrast, Jurczyk et al.[60] successfully achieved a reduction in crystallinity by incorporating oligoPHB particles into P3HB and thus also an increase in elongation and strength. Farrag et al.[61] show an improvement in thermal stability and an increase in barrier properties for starch particles in starch film.

In this work, microparticles of PHBV are used as fillers. PHBV microparticles are already used as drug release systems, vaccine engineering applications but also as purification of recombinant proteins,[62,63] or as protective coating.[64] There are different ways to produce microparticles, such as nanoprecipitation, disc rotation, electro spraying, solvent exchange, monomer polymerization, emulsion, or the miniemulsion technique, which is used in this study.[62,65] In order to scale up the production of micro- and nanoparticles to an industrial scale, Shegokar and Nakach[66] consider, for example, the use of a reliable and robust technology, the absence of contaminants, low energy consumption, safe and cost-effective production, and stability studies. A basic distinction is made between top-down and bottom-up processes. Top-down processes are, for example, wet media milling or high-pressure homogenization (HPH),[66,67] which is already approved for parenteral nutrition.[68] These robust, adaptable, reproducible manufacturing processes are characterized by their simple adaptability and their homogeneous particle size distribution.[66] Bottom-up approaches are commonly used in the pharmaceutical industry, such as precipitation, antisolvent diffusion, solvent emulsification, spray drying, etc.[66,69] These methods provide the advantage of being able to encapsulate substances and thus can be used as release systems. However, the upscaling process is more sensitive, small changes can lead to strong product-to-product variations, reproducibility can be limited, and organic solvents are also necessary for implementation.[66] Here, continuous processing approaches are becoming increasingly popular to minimize batch-to-batch differences.[67] Hoogendijk et al.[70] and von Bomhard et al.[71] have described the feasibility of a continuous production of an emulsion solvent evaporation technique, while Kakkar et al.[72] described the scale-up possibilities and limitations for a microemulsification technique for the production of lipid nanoparticles. In the end, the choice of the production method is influenced by the requirements of micro- and nanoparticles. In this work, the particles are produced by using the miniemulsion evaporation technique. In this technique, the polymer is dissolved in the solvent and mixed with a polar aqueous phase containing an emulsifier.

https://doi.org/10.1021/acsomega.4c05957
ACS Omega 2024, 9, 51073−51088

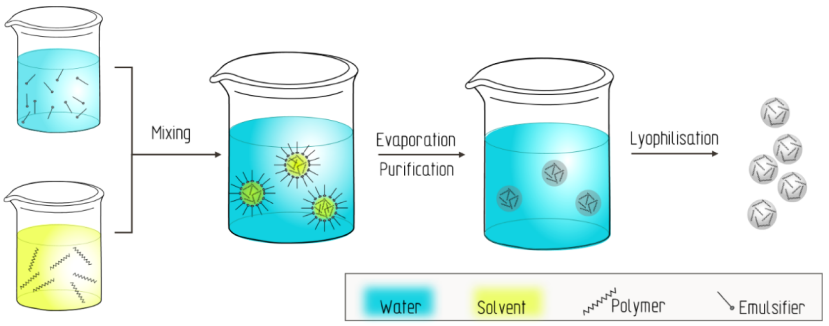

Figure 1. Miniemulsion-solvent-evaporation technique.

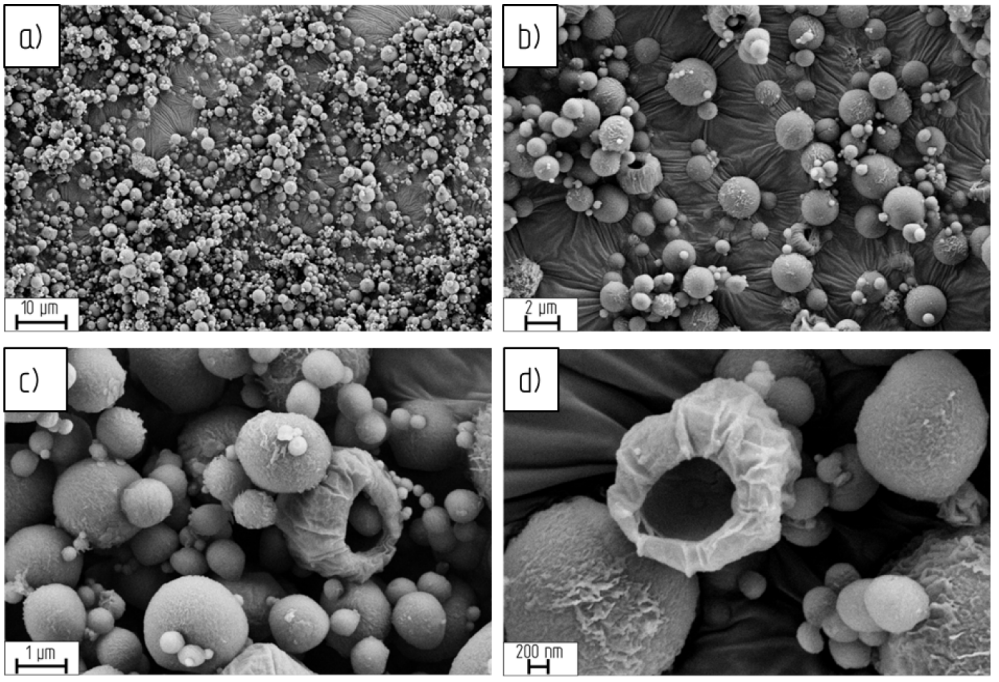

Figure 2. SEM images of PHBV microparticles with different magnifications (a) 3.0 k, (b) 10.00 k, (c) 30.00 k, and (d) 50.00 k.

Both phases are stirred to form an emulsion by external energy input.[73] Due to local polarity differences between the two phases, micelles of the polar phase are formed in which the polymer chains accumulate.[74] The resulting emulsion with the polymer droplets must have sufficient stability to prevent disintegration processes during further particle production.[75−77] The particles precipitate by evaporation of the solvent and are then separated from the emulsifier by centrifugation.[78] The resulting properties are influenced with regard to their physico-chemical characteristics of the particles such as porosity sphericity size and dispersity surface appearance and shape[79] by various factors such as molecular weight, polymer and emulsifier concentration, and energy input.[80,81]

In biocomposites, PHA particles are mainly found in the medical sector,[62] where they are being researched in creams as UV protection[82] or skin exfoliation[83] or injectable scaffolds for tissue regeneration.[84] The possibility of encapsulating antioxidant, antimicrobial, or anti-inflammatory substances in the PHA particles and achieving a targeted release make them interesting components of active materials or drug release systems.[62] However, applications have so far been limited to soft composites such as those based on hydrogels for drug carriers,[85−87] although the encapsulation of a wide variety of substances is also being promoted for other applications, such as in the packaging sector.[52,88,89]

The PHBV microparticles produced and characterized in this study are incorporated into the PHBV matrix using industry-related melt production processes. In a previous study,[90] the production of self-reinforced PHBV films with PHBV particles was successfully demonstrated using laboratory-scale solvent casting. In contrast to the production of the materials in small quantities, this study aims to provide insights into manufacturing techniques that are easily scalable to the industrial level with conventional processing methods in order to avoid additional investment costs and thus lower the inhibition threshold for the use of these composites. The composites produced with different particle concentrations are tested extensively for their thermal, mechanical, dynamic-mechanical, and barrier properties in order to assess a possible future application as a new, suitable material in the packaging industry.

MATERIALS AND METHODS

Materials. PHBV biopolymer with 12 wt % hydroxyvalerate (3HV) content (Mw: 240.000) and 10 wt % of citric acid

https://doi.org/10.1021/acsomega.4c05957
ACS Omega 2024, 9, 51073−51088

plasticized pellets was purchased from Goodfellow (Cambridge, UK). Sodium dodecyl sulfate (SDS) and dichloromethane solvent (DCM) with 99.9% of purity were purchased from Scharlab, Spain. The water used in both techniques and washing was purified on a Milli-Q ultrapure system (Millipore, Molsheim, France).

Methods. *Preparation of Microparticles.* A miniemulsion-evaporation technique according to Farrag et al.[91] was used to produce PHBV particles. It is schematically illustrated in Figure 1 and is described briefly in the following. The organic phase containing 1 wt % of the PHBV was dissolved in DCM by magnetic stirring and ultrasonic treatment. Then, the aqueous phase with 5 wt % SDS as emulsifier was mixed with the organic phase using mechanic stirring in a closed container for 1 h. In order to remove the solvent, the container was opened and stirred at 40 °C overnight to evaporate the DCM completely. Subsequently, the emulsifier was separated by centrifugation at 9000 rpm for 20 min and washing under the same conditions before the water was removed by lyophilization.

Preparation of the Biocomposites. Self-reinforced biocomposites with particle content of 1, 3, and 5 wt % PHBV particles were produced and labeled PHBV1MP(PHBV), PHBV3MP(PHBV), and PHBV5MP(PHBV), respectively; a control sample (PHBV) without particles was prepared with the same parameters. The PHBV was dried at 70 °C for 24 h prior to compounding. Extrusion was performed by a twin-screw extruder (Haake Force Feeder Minilab II, UK) with conical, counter-rotating screws and an integrated backflow channel. A processing temperature of 165 °C with a rotation speed of 60 rpm and a circulation time of 7 min was chosen. The injection was performed by using a mini-injection molding device (Thermo Scientific HAAKE MiniJet II, Karlsruhe, Germany). The pistol cylinder temperature was 165 °C, and the mold temperature was 50 °C with an injection pressure of 800 bar and a holding time of 10 s and a post pressure of 500 bar for 5 s. Dumbbell-shaped specimens according to DIN EN ISO 527-2, 5A were produced. Films of approximately 100 μm were manufactured by a heating press IQAP-LAB PL-15 (IQAP Masterbatch Group S.L., Barcelona, Spain). In the first step, the biocomposites were melted at 165 °C for 5 min and 8 kN, and then, the film was pressed with a mold for 3 min with 30 kN and finally cooled for 5 min and 8 kN.

CHARACTERIZATION

Scanning Electron Microscopy (SEM). The images of the microparticles were taken with a JEOL-JSM 7200F FESEM device (Jeol, Tokyo, Japan). The samples were sputtered with palladium, and an accelerating voltage of 5 kV was used. To perform a quantitative analysis, all particles of a representative image (Figure 2b) were analyzed with ImageJ.

Thermogravimetric Analysis (TGA). The TGA was conducted on the PerkinElmer TGA 4000 (PerkinElmer Spain SL, Madrid, Spain) apparatus to determine the thermal stability of the prepared samples. Approximately 10 mg of material was loaded in an aluminum pan. The sample was heated from ambient temperature to 500 °C at 10 °C/min under 20 mL/min N_2 flow. The temperature at 1% weight loss T_{99} is shown. The temperature of the maximum degradation rate was calculated at the DTG peak maximum (T_{max}). The residual weight was measured at the temperature of 450 °C. For the calculations, the software OriginPro 8 was used.

Differential Scanning Calorimetry (DSC). Thermal transitions of the composites were examined by a PerkinElmer Pyris Diamond/DSC 7 instrument (PerkinElmer Spain SL, Madrid, Spain) using the power compensation principle under nitrogen flow (80 mL/min) and liquid nitrogen-controlled cooling. Samples were placed in aluminum-sealed crucibles and heated from ambient temperature to 210 °C at a heating rate of 10 K/min (first heating scan), then maintained for 1 min at 210 °C, cooled rapidly at 30 K/min to −50 °C, equilibrated at −50 °C for 2 min, and heated up again to 200 °C at 10 K/min (second heating scan). The first and second heating scans examine the thermal behaviors of the samples with and without previous thermal history, respectively. The degree of crystallinity X_c of the samples was determined from the second melting enthalpy values according to the following equation:

$$X_c = \frac{\Delta H_m}{\Delta H_m^{0} w}^{*} 100$$

where ΔH_m is the second melting enthalpy of the polymer matrix, w is the polymer weight fraction of PHBV in the sample, here, 90% was calculated for raw PHBV in accordance with the manufacturer's material specification, and ΔH_m^0 is the melting enthalpy of pure crystalline PHBV (ΔH_m^0= 109 J/g).[18,92] The crystallinity of the first melting peak X_{c1} and the second melting peak X_{c2} and the total crystallinity X_c as sum of both were calculated. The analysis was realized with OriginPro 8 software.

Tensile Test. The mechanical properties were investigated as described in ASTM D 638-91 on dumbbell-shaped specimens using an Instron 5566 universal testing machine (Instron Canton, MA). The analysis was done by Bluehill software. Eight specimens of each material were tested at a cross head speed of 5 mm/min and an initial gauge length of 40 mm. Nominal stress at break (σ_b), nominal elongation at break (ε_b), and Young's modulus (E) were calculated from resulting stress−strain curves. The average value ± standard deviation of the eight samples is given in the table. Tensile strain was monitored over the pathway of the axes.

Dynamic Mechanical Analysis (DMA). Dynamic mechanical analysis (DMA) was performed in three-point bending mode with PerkinElmer DMA 7. The specimens were heated from −50 to 120 °C at a heating rate of 5 K/min, while a static force of 250 mN and a dynamic force of 200 mN at a frequency of 1 Hz were applied. The analysis was done by using the software OriginPro 8.

Polarized Optical Microscope (POM). An optical microscope in a transmission setup (Leica DM 2500 M, Leica Microsystems GmbH, Germany) was used to investigate the crystallization process of the samples. For this test, it was equipped with a Linkam hot stage. The samples were cut into thin slices with a thickness of 20 μm. Samples were heated from ambient temperature to 200 °C at a heating rate of 20 °C/min and maintained for 2 min to eliminate any crystals. The specimen was then cooled at a rate of 5 °C/min until 50 °C. Images were taken in a molten state at 210 °C. Furthermore, videos were taken throughout the crystallization period.

Transmission Electron Microscopy (TEM). Transmission electron microscopy (TEM) images were taken with a JEOL-JEM 2010 (JEOL Inc., USA). It was operated at an accelerating voltage of 100 keV. In this regard, samples were

https://doi.org/10.1021/acsomega.4c05957
ACS Omega 2024, 9, 51073−51088

cut byultramicrotome Leica Ultra Cut R with cryo-chamber Leica EM FCS (Austria) with a thickness of 80 nm.

Barrier Tests. The films, prepared in the heating press of around 110−120 μm thickness, were tested regarding their barrier properties.

The oxygen permeation measurements were performed according to ASTM DIN 3985 with the Mocon OX-TRAN model 1/50 G apparatus (Mocon, USA) at 23 °C with 1% relative humidity (RH) under 2.4 bar of pressure with a testing area of 5 cm^2. Nitrogen was used as the carrier gas with a pressure of 2.4 bar. Tests were performed until obtaining a steady line for the oxygen transmission rate under continuous mode (OTR, in $cc(m^2day)^{-1}$).

The water vapor transmission rate (WVTR) was measured with a Permatran-W, model 1/50 G, Mocon equipment (Mocon Inc., USA) complying with the ASTM E-398 standard. Masks with a 5 cm^2 test area were used for putting samples in the cell of the equipment at 37.8 °C. Relative humidities of 10 and 100% were applied in two sides of the films as the driving force of the test. The WVTR was calculated by counting the passing molecules carried to the counting chamber of the equipment with nitrogen gas as a carrier, which was purged continuously during the test with nitrogen at 2.0 bar. Tests were performed until obtaining a steady line for the water vapor transmission rate under continuous mode (WVTR, in $g(m^2day)^{-1}$).

Statistical Analysis. The results of some of the tests performed are given as average values ± the standard deviation. A statistical analysis of the results of the tensile and barrier tests was performed using OriginPro 8. First, the values were tested for normal distribution using the Shapiro−Wilk test, and then, a one-way ANOVA analysis was performed using Tukey's test for means comparisons and Levene's test for homogeneity of variance. If the homogeneity of variance was significant, then a Kruskal−Wallis test was performed to test the significance of the values. The significance level for all statistical analyses was $\alpha = 0.05$.

RESULTS AND DISCUSSION MICROPARTICLES

In this first part of the article, the results of the manufactured PHBV microparticles in comparison to the neat polymer are presented.

Scanning Electron Microscopy Analysis. Controlling the size and morphology of the microparticles is crucial for the resulting properties of the particle composite for the following incorporation of the particles into the matrix. To gain a better understanding of the PHBV microparticles, SEM images were taken (Figure 2). The particles are well-separated with a rather smooth surface. Although most of them are spherical, some hollow particles (capsules) can also be found as shown in Figure 2c,d. The particle diameters are in the nano- to micrometer range and reach up to about 5 μm. During the more precise analysis of the images with ImageJ, as shown in Figure 3, the particle diameters were measured. The measurement showed a monomodal distribution, which resembles a log-normal distribution (dashed curve). Accordingly, the particles had a mean diameter of 0.44 μm, with a standard deviation of 0.77 μm.

The particles showed similar morphology and size to those reported in the literature.[73,90,91,93,94] Malmir et al.[90] produced PHBV particles using the miniemulsion evaporation technique with SDS as an emulsifier, resulting in a similarly smooth surface. Zalloum et al.[94] observed a rougher surface with a similar size distribution for prepared PHBV particles. Senhorini et al.[93] also produced similar diameters but with a rougher surface with more pores, while Pettinelli et al.[87] produced slightly smaller and smoother PHBV particles. Leimann et al.[76] showed smaller, agglomerated nanoparticles, while Barboza et al.[95] and Volant et al.[79] showed particles with an average diameter of 5 and 25 μm, respectively. Farrag et al.[91] also produced similar particles using SDS and poly(vinyl alcohol) (PVA) as emulsifiers, and they showed some hollow particles. Im et al.[96] and Mahaling and Katti[97] investigated hollow polymer particles and saw the polymer concentration gradient during extraction of the solvent as the basis for this phenomenon. Im et al.[96] emphasized that this can be observed with larger P3HB particles. Compared to the P3HB granules in living cells as described and investigated by Vadlja et al.,[98] the produced microparticles are significantly larger.

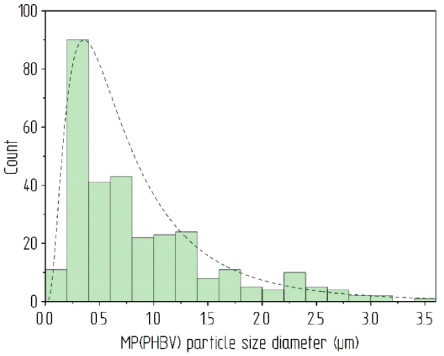

Figure 3. Distribution of particle diameter of PHBV microparticles by ImageJ with a log-normal distribution curve (dashed line).

The size and morphology of the particles are influenced by many factors in the miniemulsion-solvent technique. Some of these conditions have already been investigated in the literature. For example, Farrag et al.[91] showed smaller particles with a smaller distribution for lower polymer solution concentrations or higher surfactant concentrations. Maia et al.[99] demonstrated the influence of surfactant concentration and processing conditions such as temperature and solvent composition. Leimann et al.[76] and Volant et al.[79] showed a dependence of the molar mass and the complexity of the PHA molecular chains on the size of the particles. You et al.[100] presented in a comprehensive study the influence of the polymer concentration, stirring speed, and surfactant content on PHBV particles with dimethylisosorbide as the solvent. According to the literature, porosity is mainly influenced by the evaporation rate.[99] Besides that, Farrag et al.[91] also observed a correlation of the porosity with the polymer concentration. The roughness of the surface was influenced by a variety of factors such as the stirring speed, the choice of surfactant and additives, and the molar mass and complexity of the molecular chains and thus the crystallinity of the particles.[79,91,94] Zalloum et al.[94] described a local gelatinization for PVA as a surfactant which binds to the surface of the microparticles and influences properties of the microparticles such as hydrophobicity and degradation properties. However, this behavior has not yet been proven for SDS. Nevertheless, Koosha et al.[101] showed that despite cleaning steps in the solvent evaporation process during the P3HB particle preparation, small fractions of SDS remained on their surface.

Thermogravimetric Analysis. Since thermal behavior affects the processing window and the materials areas of

https://doi.org/10.1021/acsomega.4c05957
ACS Omega 2024, 9, 51073−51088

application, the thermal stability was investigated here (Figure 4 and Table 1). In the present study, the thermal stability of

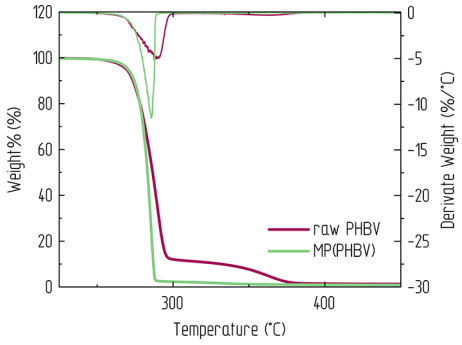

Figure 4. Thermogravimetric analysis of PHBV microparticles and raw PHBV, weight loss curves, and first derivate.

Table 1. TGA Results of Raw PHBV and PHBV Microparticles[a]

TGA	T_{99} [°C]	T_{max} [°C]	Residual weight [wt %]
Raw PHBV	255.1	287.5	1.2
MP(PHBV)	256.8	285.6	0.9

[a]Temperature of 1% weight loss T_{99}, temperature of maximal degradation rate T_{max}, residual weight at 450 °C.

the particles has increased slightly compared to pure PHBV. The start of the degradation at 1% weight loss was observed at 255.1 °C for pure PHBV and 256.8 °C for the PHBV microparticles. The second degradation peak of the raw PHBV could correspond to the plasticizer, which according to the manufacturer is a citric acid ester, in the weight percentage of about 10 wt % and with a T_{max} of 363 °C.[102] Due to the purification of the PHBV during the manufacturing process, these plasticizers were probably eliminated from the particles and therefore responsible for the absence of the second degradation phase. This could also come along with the smaller residual weight at the 450 °C where raw PHBV has 1.2 wt %, while the PHBV particles have just 0.9 wt %. The findings of the TGA confirm the observations of other authors of no significant or only slight tendencies toward a reduction in thermal stability between the starting material and the particles. While Senhorini et al.[93] observed no change in the onset temperature of degradation, Bouza et al.[73] showed in their work for PHBV pellets a temperature set of 285 °C which slightly decreased to 279 °C for PHBV particles. They also found for the raw PHBV material a two-step degradation, while the decomposition of the PHBV particles took place in one step. Rastogi and Samyn[64] reported similar results. They attributed this to the larger free surface area due to the submicrometer size of the particles, which was less thermally stable compared to the original compacted starting pellet.

Differential Scanning Calorimetry. The materials' melting and crystallization behavior was assessed by means of differential scanning calorimetry (DSC). Figure 5 shows the composites' first heating and first cooling curves, respectively. Two melting areas were found for both, the original PHBV polymer and the PHBV particles produced. As can be seen in Tables 2 and 3, the prepared particles showed slightly higher melting temperatures of 153.3 and 167.0 °C for the first and second melting peaks, respectively, compared to raw PHBV, which showed 150.3 and 162.1 °C, respectively. This is

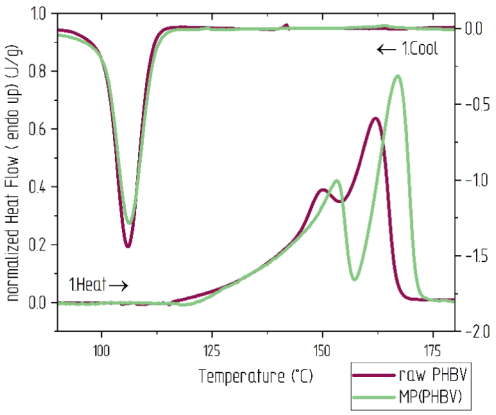

Figure 5. DSC curves of 1. heating and 1. cooling of the raw PHBV and PHBV microparticles.

accompanied by slightly higher melting enthalpies of 71.6 J/g of PHBV microparticles compared to 68.3 J/g of pure PHBV. However, the calculated crystallinity for the two materials is very close to each other, based on the fact that the crystallinity for the microparticles was calculated without the weight proportion of the plasticizer based on the results of the TGA tests. The crystallization temperatures are almost the same for raw PHBV and MP(PHBV).

The presence of a split endothermic melting behavior for PHBV has already been described in the literature for PHBV[90,103−105] and for PHBV particles.[64,73,79] The possible reason could be a complex superposition of different effects. According to recent investigations, the different thicknesses of the spherulite lamellae and the size of the unit cells[105−107] had a major influence. However, recrystallization processes and different morphologies could also be involved. Only a crystalline reorganization was excluded by Volant et al.[79] and Senhorini et al.[93]

Maia et al. also observed an increase in the melting temperatures of the PHBV microspheres compared to the raw material.[99] Rastogi and Samyn[106] mentioned the higher chain mobility for the microparticles, which enabled a higher degree of order in the spherulites and resulted in higher melting enthalpies for P3HB microparticles in comparison with the neat P3HB. Cai et al.[108] described lower melting temperatures for poly(3-hydroxybutyrate-*co*-3-hydroxyhexanoate) (PHB3HHx) with a higher content of more complex 3-hydroxyhexanoate (3HHx) groups. Volant et al.[79] also mentioned the lateral side chain size as an influencing factor for crystallinity. Furthermore, they showed a correlation between the roughness of the particles and the crystallinity of the particles through investigations with the AFM and FTIR. In this work, the treatment of the polymer chains during the preparation of the PHBV microparticles could have led to a purification of the plasticizer, as described above in the TGA, and a slight loss of complexity in the molecular chains compared to the raw material, which would favor crystallinity.[64]

RESULTS AND DISCUSSION BIOCOMPOSITES

This second part of the review is dedicated to the findings on the PHBV composites resulting from the extrusion and injection molding of the manufactured microparticles within a PHBV matrix. Results of biocomposites with 1, 3, and 5 wt %

https://doi.org/10.1021/acsomega.4c05957
ACS Omega 2024, 9, 51073−51088

Table 2. DSC Analysis of Raw PHBV and PHBV Microparticles in First Heating

1. Heating	T_{m1} [°C]	ΔH_{m1} [J/g]	X_{c1} [%]	T_{m2} [°C]	ΔH_{m2} [J/g]	X_{c2} [%]	X_c [%]
Raw PHBV	150.3	33.8	31.6	162.1	34.5	35.2	66.1
MP(PHBV)	153.3	35.0	32.1	167.0	36.6	33.6	65.7

Table 3. DSC Analysis of Raw PHBV and PHBV Microparticles in First Cooling

1. Cooling	T_{c1} [°C]	ΔH_{m1} [J/g]
Raw PHBV	105.8	−60.8
MP(PHBV)	106.3	−59.3

of PHBV microparticles are shown and compared to the neat matrix material.

Microscopic Analysis. First, SEM images were taken of the cryo-fractured sample surface to check whether the PHBV microparticles have withstood melt production by extrusion and injection and if they can be detected. Figure 6 shows

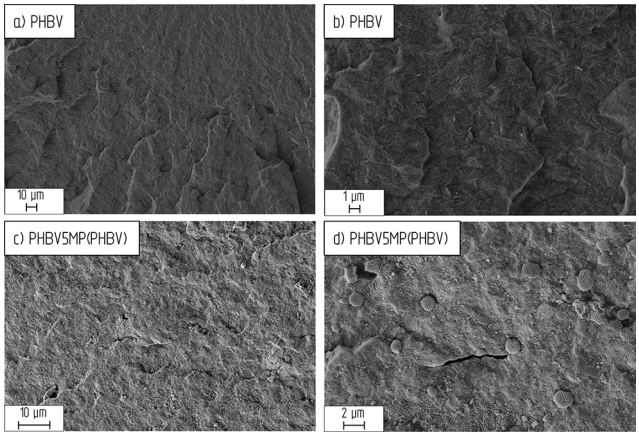

Figure 6. SEM images of composites (a) PHBV at 1.00 k ×, (b) PHBV at 10.00 k ×, (c) PHBV5MP(PHBV) at 3.00 k ×, and (d) PHBV5MP(PHBV) at 10.00 k ×.

images of PHBV and PHBV5MP(PHBV). Spherical particles with a diameter of about 1 μm can be recognized for the particle composite. However, the analysis of the particles also identified larger particles that are not visible in the microscopy images; this may be due to the degradation of the larger particles during melt processing. The applied shear forces and increased temperatures could promote degradation of the particles. However, there are no obvious signs of good bonding to the matrix, but on the other hand, this cannot be excluded as the particles and matrix are made of the same material and thus can just be clearly seen at some parts of the composite as can be seen in Figure 6c,d.

To give a deeper understanding of the material, TEM images shown in Figure 7 were taken. Spherical particles could be found in the matrix at all concentrations. The hollow particles, as described above, can be seen in Figure 7d,e, are clearly identified here as PHBV particles. Compared with the SEM, however, much smaller particles of less than 1 μm in diameter can be measured here. For larger particle contents for PHBV5MP(PHBV), agglomerates are visible, in contrast to the SEM images. Malmir et al.[90] also show TEM images of the biocomposites produced with solvent casting with PHBV microparticles, but they cannot detect any spherical particles.

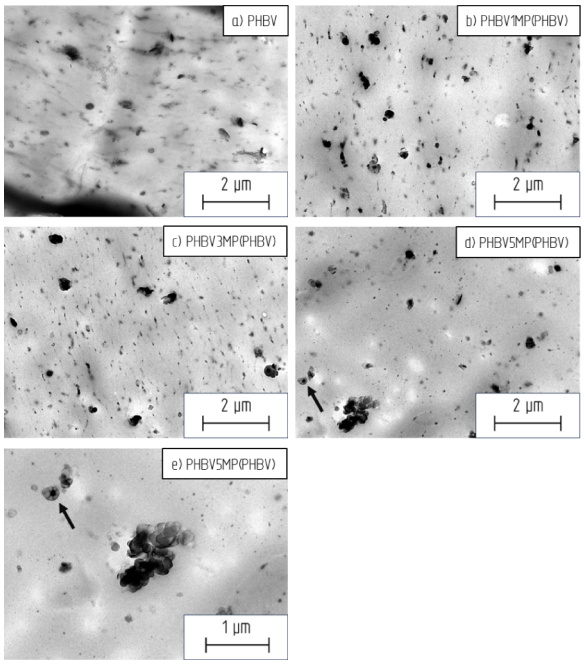

Figure 7. TEM images of composites: (a) PHBV at 15000×, (b) PHBV1MP(PHBV) at 15000×, (c) PHBV3MP(PHBV) at 15000×, (d) PHBV5MP(PHBV) at 15000×, and (e) PHBV5MP(PHBV) at 30000×.

Differential Scanning Calorimetry. The thermal effects of the particles on the biocomposites with a PHBV matrix were investigated using DSC (Figure 8, Tables 4 and 5). Two melting areas were found for all of the samples. The presence of a split endothermic melting behavior for PHBV was already described above and in the literature.[90,103,104] Possible causes of double melting behavior include (a) melting, recrystallization, and remelting during heating; (b) the presence of more than one crystal modification; (c) different morphologies, and (d) relaxation of the rigid amorphous fraction.[79,103] Zhu et al.[105] studied recently PHBV regarding its bimodal melting behavior and showed that thinner lamellae with larger unit cells are melted in the first melting area and thicker spherulites with smaller unit cells are melted in the second melting area. As an explanation, they suggested that the thinner, thermally less stable lamellae had a uniform structure with 3HV units, while the thicker lamellae reflected a sandwich structure with partial inclusion of 3HV units. However, the work revealed no evidence of a structural change due to recrystallization.

The analysis of the DSC data showed a very slight increase in the melting temperatures for the incorporation of the PHBV microparticles by approximately 2 °C as well as a slight widening of the melting range. In addition, a higher enthalpy in the first peak from 48.8 J/g for PHBV to 58.0 °C for PHBV3MP(PHBV) and an increased crystallinity of about 10% can be observed. Xu et al.[109] observed an increase in crystallization and melting peaks as well as an extension of the melting range for self-induced nucleation by P3HB in PHBH. This was attributed to improved crystallization ability and

https://doi.org/10.1021/acsomega.4c05957
ACS Omega 2024, 9, 51073−51088

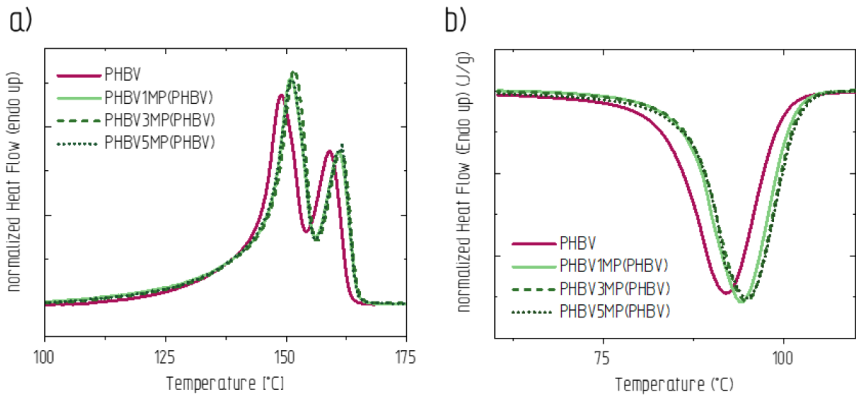

Figure 8. DSC curves of the PHBV and biocomposites: (a) second heating scan and (b) first cooling scan.

Table 4. DSC Data of First Cooling of PHBV and Biocomposites

1. Cooling	T_c [°C]	ΔH_C [J/g]
PHBV	91.9	−54.0
PHBV1MP(PHBV)	93.9	−52.4
PHBV3MP(PHBV)	94.9	−53.5
PHBV5MP(PHBV)	94.9	−55.1

quality, which increased the thickness of PHBH lamellae and made the crystals more perfect.

Understanding the nonisothermal crystallization behavior of the material is essential for melt processing. It can be seen that the crystallization ranges and their peaks for the particle composites are shifted to higher temperatures. For example, the crystallization peak for PHBV3MP(PHBV) is at 94.9 °C, while for PHBV, it is only at 91.9 °C. Crystallization involves nucleation and crystal growth processes, which can be influenced by various factors, such as the dispersion of the particles, the bonding between the matrix and filler, or chain mobility.[110] The earlier crystallization in the composites indicates that the PHBV particles act as heterogeneous nucleating agents, which reduce the activation energy for crystallization. Malmir et al.[90] and other authors[103,110,111] described similar trends and attributed this to smaller and more crystalline domains formed due to heterogeneous nucleation.

Thermogravimetric Analysis. The composites produced by melt processing were also investigated by thermogravimetric analysis. As can be seen in Figure 9 and Table 6, the addition of microparticles resulted in slightly faster thermal decomposition of the biocomposites compared to pure PHBV. For example, the temperatures at 1 wt % weight loss for PHBV5MP(PHBV) are 255.4 °C, while the thermal decomposition of pure PHBV starts at 263.2 °C. As described above for raw PHBV, a second decomposition peak is also measured here for both the pure PHBV and the biocomposites, which could correspond in its weight percent (∼10 wt %) and its decomposition temperature of 363 °C to a citric acid ester, which is added as a plasticizer according to the manufacturer's specifications.

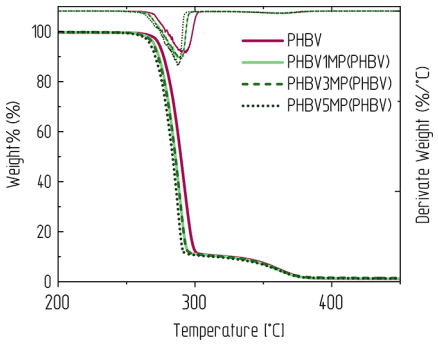

Figure 9. TGA curve of the biocomposites.

Table 6. TGA Results of Biocomposites[a]

TGA	T_{99} [°C]	T_{max} [°C]	$\text{Weight}_{Residual}$ [wt %]
PHBV	263.2	292	1.0
PHBV1MP(PHBV)	259.4	290	1.1
PHBV3MP(PHBV)	258.5	290	1.4
PHBV5MP(PHBV)	255.4	287	1.2

[a]Temperature of 1% weight loss T_{99}, temperature of maximal degradation rate T_{max}, residual weight at 450 °C $\text{weight}_{residual}$.

Xiang et al.[25] studied the thermal decomposition of PHBV in the relationship between the external atmosphere and the residual metal ions. They prove that PHBV with low molecular weight and a crotonate end group at the end was generated by random chain scission triggered by the reaction of β-elimination and α-deprotonation.[112] Subsequently, the crotonic acid and a new crotonyl chain end were generated with a drastic reduction in molecular weight. Here, they further showed acceleration by the remaining calcium ions in the PHBV.

Table 5. DSC Data of Second Heating of PHBV and Biocomposites

2. Heating	T_{m1} [°C]	ΔH_{m1} [J/g]	X_{c1} [%]	T_{m2} [°C]	ΔH_{m2} [J/g]	X_{c2} [%]	X_c [%]
PHBV	149.1	48.8	44.8	159.1	19.2	17.6	62.4
PHBV1MP(PHBV)	151.1	51.3	47.6	160.9	19.1	17.7	65.3
PHBV3MP(PHBV)	151.7	58.0	54.8	161.4	18.8	17.8	72.6
PHBV5MP(PHBV)	151.1	56.6	54.6	161.6	19.9	19.2	73.8

https://doi.org/10.1021/acsomega.4c05957
ACS Omega 2024, 9, 51073−51088

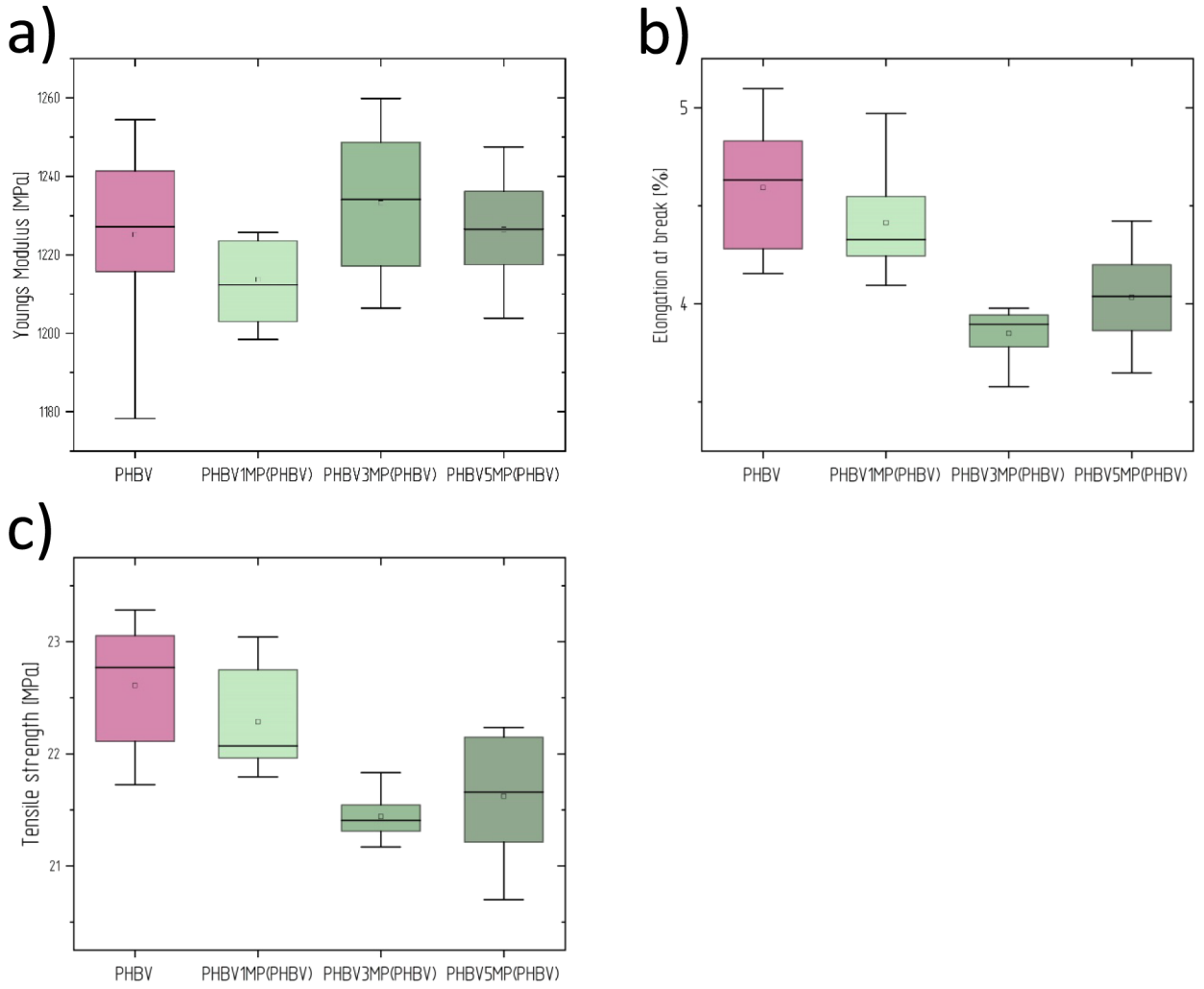

Figure 10. Tensile test, stress strain curve, and block diagrams of (a) Young's modulus E, (b) elongation at break ε_b, and (c) tensile strength ε_f.

Table 7. Results of Tensile Test-Injected Biocomposites with Mean Values and Standard Deviation

Tensile test	Young's Modulus	Elongation in F_{max}	Tensile strength	Elongation at break	Breaking stress
	E [MPa]	ε_f [%]	σ_f [MPa]	ε_b [%]	σ_b [MPa]
PHBV	1225 ± 24	4.4 ± 0.3	22.6 ± 0.6	4.6 ± 0.3	22.4 ± 0.7
PHBV1MP(PHBV)	1214 ± 10	4.2 ± 0.3	22.3 ± 0.5	4.4 ± 0.3	21.2 ± 0.6
PHBV3MP(PHBV)	1233 ± 19	3.6 ± 0.1	21.4 ± 0.2	3.8 ± 0.1	19.8 ± 0.6
PHBV5MP(PHBV)	1226 ± 14	3.8 ± 0.3	21.6 ± 0.6	4.0 ± 0.3	20.3 ± 0.6

Many studies have described a decrease in thermal stability due to the incorporation of fillers. Especially, the addition of particles with higher thermal conductivity, as they enhanced heat diffusion through the material, showed greater effects.[111,113]

Oberhoff,[114] Mysiukiewicz et al.[115] and Vanheusden et al.[116] described a strong influence of the process parameters on thermal stability, with shear forces being primarily responsible for chain shortening. They demonstrated the strong influence of viscosity as an interaction of incorporated fillers, process temperatures, and rotation speeds on thermal stability. Also in this work, the particles could lead to an increase in shear forces during extrusion, which could lead to a shortening of the chain length and, therefore, to an earlier thermal degradation.

Tensile Test. The injection-molded samples were examined using the tensile test to determine their modulus, strength, and elongation. Figure 10 shows the results of the mechanical properties of the tensile test plotted as a box chart. Table 7 summarizes the average values and their standard deviations. Statistical analysis showed a slight reduction in strength and a decrease in ductility, while the elasticity did not change significantly. As the variance of homogeneity according to Levene was significant (0.04) for the tensile strength, a Kruskal–Wallis test was also carried out for this parameter, which confirmed a significant change in the tensile strengths of the materials. The greatest effect was achieved with 3 wt % PHBV microparticles, at which the composites showed the strongest decrease in mechanical properties, leading to embrittlement, which is associated with the increased crystallinity shown in the DSC. At higher particle contents, agglomeration of the particles occurs as seen in the TEM, which counteracts this. A decrease in mechanical properties

https://doi.org/10.1021/acsomega.4c05957
ACS Omega 2024, 9, 51073−51088

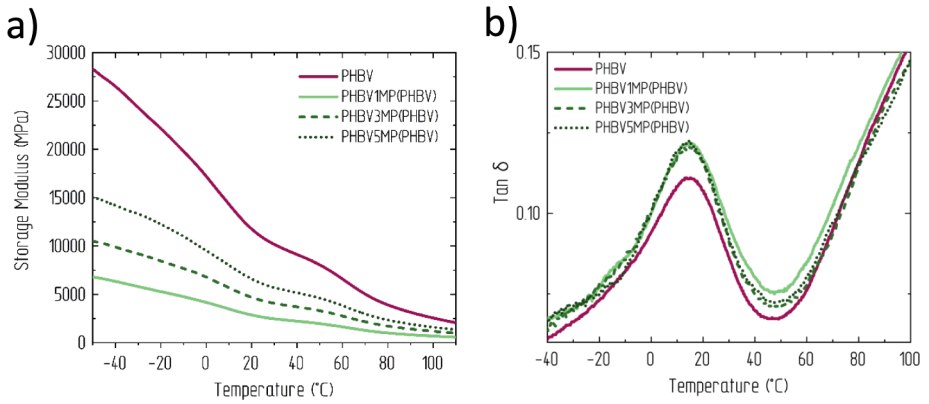

Figure 11. DMA curves of biocomposites: (a) storage modulus and (b) tan δ.

was also observed by other authors. Mazur et al.[117] showed no clear influence of CuO particles on the mechanical properties of PHBV. Najah et al.[118] described a decrease in strength and ductility for calcium phosphate-PHA composites, which they attributed to dispersion and poor bonding of the particles. Jurczyk et al.[60] showed a decrease in mechanical and thermal properties for self-reinforced PHB with clPHB. Xu et al.[109] mixed PHB in PHBH as a nucleating agent and observed a higher strength of the materials with increased crystallinity. Tamiya et al.[119] showed poorer elongation and strength for PHBV composites with silicate particles and attributed this to poor bonding. Bossu et al.[120] investigated different process temperatures for PHBV and showed a strong decrease in mechanical properties at high temperatures due to a separation of the P3HB and P3HV domains, which can also increase due to self-heating. A decrease in the mechanical properties due to chain shortening caused by decomposition processes during melt production, as previously described, is also conceivable. Many factors influence the mechanical properties of composite materials. The main difference in the given literature between conventional fillers and nanofillers was that nanosized materials had a much larger surface area and therefore a larger interfacial area per unit volume. Therefore, nanocomposites showed an improvement in mechanical properties, but a common problem is the limitation of particle content due to the formation of agglomerates due to poorer dispersion.[121] However, the peculiarity lies in the increased crystallinity of the composites, which does not lead to a higher modulus as expected but only to an embrittlement of the composites. At higher particle contents, agglomeration could occur, which counteracts this. In order to better understand this phenomenon, DMA was carried out.

Dynamical Mechanical Analysis. In order to understand the dynamic mechanical mechanisms, a DMA was carried out in a bending test setup. The results are shown in Figure 11 and Table 8. Lower storage moduli of the biocomposites can be seen over the entire temperature range, with greater differences at temperatures below the glass transition temperature, which converge as the temperature increases. One wt % of the PHBV particles have the greatest effect, causing a reduction of around 70% at 30 °C compared to the pure PHBV. The modulus is a value for the stiffness of the sample, i.e., conversely the chain mobility. The lower the value, the higher the degree of freedom of the chains. Therefore, in the glass transition region, a strong loss of modulus for all polymers has been seen due to the weakening of the intermolecular interactions by the alpha relaxation of the amorphous phase.[113] The incorporation of the particles also resulted in lower moduli, which were accompanied by an increased phase shift tan δ, i.e., an increased damping capacity of the biocomposites due to the increased energy dissipation.[103] One possible explanation for this could be a change in the crystal structure. On the other hand, as already discussed, higher particle contents could lead to agglomeration, which counteracted the refinement of the crystal structure and limited internal structure movements.[122] Brandolt et. al[110] also reported a decrease in modulus with an increase in the phase shift for nanoclays and plasticizers in PHBV and also attributed the higher chain mobility for the nanocomposites.

Table 8. DMA values of biocomposites: storage modulus and phase shift tan δ

DMA	Modulus [MPa]			tan (δ)	
	at 10 °C	at 30 °C	at 70 °C	T_g [°C]	tan (δ)
PHBV	14052	9989	5027	14,8	0,11
PHBV1MP(PHBV)	3969	2863	1441	14,6	0,12
PHBV3MP(PHBV)	4628	3321	1730	14,7	0,12
PHBV5MP(PHBV)	5951	4334	2196	14,9	0,12

Polarized Optical Microscopy. In order to understand the crystal structure, images were taken with POM, which are shown in Figure 12. The images were taken after complete crystallization at 85 °C. The examination shows higher crystallization temperatures for the biocomposites with

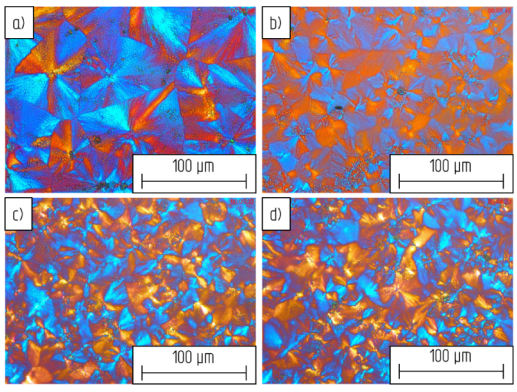

Figure 12. POM Images of biocomposites after cooling from melt at 85 °C: (a) PHBV, (b) PHBV1MP(PHBV), (c) PHBV3MP(PHBV), and (d) PHBV5MP(PHBV).

https://doi.org/10.1021/acsomega.4c05957
ACS Omega 2024, 9, 51073−51088

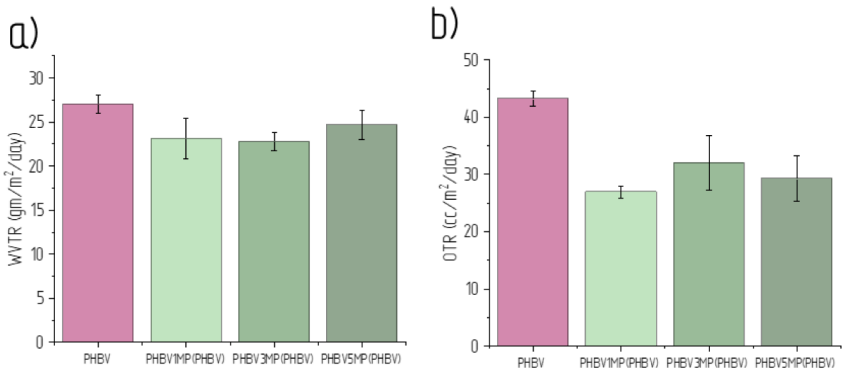

Figure 13. Barrier tests of biocomposite films against (a) water vapor transmission rate and (b) oxygen transmission rate.

PHBV particles, shown in Figure 12b–d compared to neat PHBV, shown in Figure 12a. By incorporating the particles, a reduction in the size of the spherulites with significantly more nucleation nuclei can be observed, resulting in more interfaces between the spherulites. This confirms the findings from DSC and DMA analyses. However, due to the diffuse images, no major differences can be observed between the biocomposites with different particle contents with regard to the size of the spherulites or their perfection. The semicrystalline random copolymers are isodimorphic, which implies the cocrystallization of the two monomer units in the PHB homopolymer lattice (Bluhm et al. 1986). They are composed of spherulites, which are characterized by crystalline domains surrounded by the amorphous phase, wherein the amorphous phase is characterized by a continuum, i.e., a broad distribution of the rigid and mobile phase (Esposito et al. 2016). In the literature, the reinforcing effect of the particles was also observed by the formation of more spherulites and higher crystallization temperatures due to heterogeneous nucleation.[109,111] The earlier crystallization due to the energetic situation in the composites was already observed in the investigation using DSC and can be confirmed here. Malmir et al.[90] described for PHBV composites produced by solvent casting a faster growth rate, which they have demonstrated in other investigations as well. Moreover, da Costa et al.[103] related the differences in perfection and size of the spherulites to the agglomeration of the fillers and to the two endothermic melting peaks of the DSC. The results therefore confirm the DMA and DSC assumptions of a higher nucleation density and smaller spherulites.

Barrier Test. Good barrier properties indicate good protection against environmental influences, thus preventing the fast deterioration of the products. The permeability of oxygen and water vapor was measured as an indicator of the barrier properties, and the results are shown in Figure 13. A significant increase in oxygen barrier properties for PHBV was observed compared to the materials with incorporated microparticles according to the Tukey's test. OTR values were 35% increased for PHBV1MP(PHBV) compared to pure PHBV from 42.3 cc/m^2/day to 27.3 cc/m^2/day with $p = 0.004$. The water vapor permeability was also slightly improved for PHBV3MP(PHBV) from 26.3 to 23.3 g/m^2/day but not significantly according to ANOVA analysis with $p = 0.095$. The different intensity of the effects for water vapor versus oxygen can be attributed to the polarity of the gas molecules and their size. This allowed the water molecules to use the OH bonds as bridges to permeate through the material.[111] The diffusion coefficient was significantly lower in the amorphous phase than in the crystalline lamellae of the spherulites, which indicated that molecular migration mainly took place in these areas due to the higher free volume.[123] Due to the higher crystallinity observed in the DSC for the biocomposites with the PHBV particles, gas diffusion through the sample was hindered. Smaller spherulites and more frequent spherulite boundaries as well as the introduced PHBV particles contributed to a complicated path of the molecules through the sample,[90,103] as seen before in the POM analysis. However, it should be noted that at higher particle contents, the agglomeration of the particles counteracted this.[124]

CONCLUSIONS

PHBV microparticles with an average diameter of 3–4 μm were first produced by using the miniemulsion-evaporation technique. Compared with the PHBV raw material, they showed a slightly higher crystallinity with a slight increase in melting temperatures. Afterward, they were used as a self-reinforcing agent by incorporating them in a PHBV matrix using melt processing. The analysis by applying different techniques revealed the effect of microparticles on the properties of the composite. By use of microscopic images, small particles could be detected in the composite. It can be shown that they achieved a heterogeneous nucleation, as a result of which a higher nucleation density was determined. The mechanical properties were not strongly influenced, which is explained by opposing effects. On the one hand, increased degradation processes during melt processing due to the higher particle-induced shear forces occur, and on the other hand, there is a reinforcing effect caused by the change in the crystal structure of PHBV due to the microparticles, which was demonstrated in the POM. The finer microstructure with the higher number of spherulites and more interfaces, together with the higher crystallinity, is also shown to worsen the diffusion of permeants through the composite, resulting in improved barrier properties. This composite material has shown promise for industrially produced, sustainable, biobased, and biodegradable packaging materials of the future. In the future, the composite material could benefit from the further development of microparticles, first by realizing larger quantities by an upscale[70,72] with more efficient use of more sustainable substances[100,125] during production and second through the encapsulation of antimicrobial, antioxidant, or anti-inflammatory substances, as well as upscaling processes, e.g., in the production of contacts. In combination with the good barrier properties, interesting active packaging systems can be produced.

https://doi.org/10.1021/acsomega.4c05957
ACS Omega 2024, 9, 51073–51088

■ ASSOCIATED CONTENT

Data Availability Statement

The data are available at Mendeley Data Repository: DOI: 10.17632/szsbgmvn8r.1.

Supporting Information

The Supporting Information is available free of charge at https://pubs.acs.org/doi/10.1021/acsomega.4c05957.

POM images at different temperatures during crystallization from the melting state of PHBV biocomposites (PDF)

■ AUTHOR INFORMATION

Corresponding Author

Anja Schmidt − *Grupo de Polímeros, Centro de Investigación en Tecnologías Navales e Industriales (CITENI), Departamento de Física y Ciencias de la Tierra, Universidade da Coruña (UDC), 15471 Ferrol, Spain;* orcid.org/0000-0001-6013-6063; Email: a.schmidt@udc.es

Authors

Birgit Bittmann-Hennes − *Leibniz-Institut für Verbundwerkstoffe GmbH, 67663 Kaiserslautern, Germany*

Danny Moncada − *Grupo de Polímeros, Centro de Investigación en Tecnologías Navales e Industriales (CITENI), Departamento de Física y Ciencias de la Tierra, Universidade da Coruña (UDC), 15471 Ferrol, Spain;* orcid.org/0000-0002-4903-1460

Belén Montero − *Grupo de Polímeros, Centro de Investigación en Tecnologías Navales e Industriales (CITENI), Departamento de Física y Ciencias de la Tierra, Universidade da Coruña (UDC), 15471 Ferrol, Spain*

Complete contact information is available at: https://pubs.acs.org/10.1021/acsomega.4c05957

Author Contributions

All authors contributed to the study conception and design. Material preparation, data collection, and analysis were performed by Anja Schmidt. The first draft of the manuscript was written by Anja Schmidt, and all authors commented on previous versions of the manuscript. All the authors read and approved the final manuscript. Anja Schmidt contributed to methodology, investigation, visualization, and writing of the original draft. Birgit Bittmann-Hennes contributed to supervision, writing (review and editing), and funding acquisition. Danny Moncada contributed to methodology and investigation. Belén Montero contributed to conceptualization, supervision, writing (review and editing), and funding acquisition.

Funding

This work was partially supported by the Xunta de Galicia Government: program of consolidation and structuring competitive research units [grant number: ED431C 2023/34] and by the European Union through the project Waste2BioComp (101058654). Views and opinions expressed are however those of the authors only and do not necessarily reflect those of the European Union. Neither the European Union nor the granting authority can be held responsible for them. Funding for open access charge was given by Universidade da Coruña/CISUG.

Notes

The authors declare no competing financial interest.

Not applicable. This study does not contain any studies involving human participants and/or animals performed by any of the authors.

■ REFERENCES

(1) Sparrow, N.; Read, M. *Plastic Pellet Spill in Spain Galvanizes EU Parliament*, 2024; pp 1−6. https://www.plasticstoday.com/legislation-regulations/plastic-pellet-spill-in-spain-galvanizes-eu-parliament.

(2) Tóth, C.; Virág, Á. D.; Mészáros, L. Recycling Issues with Multilayer Packaging. *Express Polym. Lett* **2024**, *18* (4), 348.

(3) Carpine, R.; Olivieri, G.; Hellingwerf, K. J.; Pollio, A.; Marzocchella, A. Industrial Production of Poly-β-Hydroxybutyrate from CO2: Can Cyanobacteria Meet This Challenge? *Processes* **2020**, *8* (3), 323.

(4) Mukherjee, A.; Koller, M. Microbial PolyHydroxyAlkanoate (PHA) Biopolymers—Intrinsically Natural. *Bioengineering* **2023**, *10* (7), 855.

(5) Obruca, S.; Sedlacek, P.; Slaninova, E.; Fritz, I.; Daffert, C.; Meixner, K.; Sedrlova, Z.; Koller, M. Novel Unexpected Functions of PHA Granules. *Appl. Microbiol. Biotechnol* **2020**, *104* (11), 4795−4810.

(6) Khatami, K.; Perez-Zabaleta, M.; Owusu-Agyeman, I.; Cetecioglu, Z. Waste to Bioplastics: How Close Are We to Sustainable Polyhydroxyalkanoates Production? *Waste Manage* **2021**, *119*, 374−388.

(7) Lee, J.; Park, H. J.; Moon, M.; Lee, J. S.; Min, K. Recent Progress and Challenges in Microbial Polyhydroxybutyrate (PHB) Production from CO2 as a Sustainable Feedstock: A State-of-the-Art Review. *Bioresour. Technol* **2021**, *339* (June 2021), 125616.

(8) McAdam, B.; Fournet, M. B.; McDonald, P.; Mojicevic, M. Production of Polyhydroxybutyrate (PHB) and Factors Impacting Its Chemical and Mechanical Characteristics. *Polymers* **2020**, *12* (12), 2908.

(9) Kuddus, M. *Bioplastics For Sustainable Development*; Springer Singapore, 2021.

(10) Ganesh Saratale, R.; Cho, S. K.; Dattatraya Saratale, G.; Kadam, A. A.; Ghodake, G. S.; Kumar, M.; Naresh Bharagava, R.; Kumar, G.; Su Kim, D.; Mulla, S. I.; Seung Shin, H. A Comprehensive Overview and Recent Advances on Polyhydroxyalkanoates (PHA) Production Using Various Organic Waste Streams. *Bioresour. Technol* **2021**, *325* (November 2020), 124685.

(11) Chen, G. Q.; Chen, X. Y.; Wu, F. Q.; Chen, J. C. Polyhydroxyalkanoates (PHA) toward Cost Competitiveness and Functionality. *Adv. Ind. Eng. Polym. Res* **2020**, *3* (1), 1−7.

(12) Kosseva, M. R.; Rusbandi, E. Trends in the Biomanufacture of Polyhydroxyalkanoates with Focus on Downstream Processing. *Int. J. Biol. Macromol* **2018**, *107* (PartA), 762−778.

(13) Zheng, Y.; Chen, J. C.; Ma, Y. M.; Chen, G. Q. Engineering Biosynthesis of Polyhydroxyalkanoates (PHA) for Diversity and Cost Reduction. *Metab. Eng* **2020**, *58* (March 2019), 82−93.

(14) Raza, Z. A.; Abid, S.; Banat, I. M. Polyhydroxyalkanoates: Characteristics, Production, Recent Developments and Applications. *Int. Biodeterior. Biodegrad* **2018**, *126*, 45−56.

(15) Sirohi, R.; Prakash, J.; Kumar, V.; Gnansounou, E.; Sindhu, R. Bioresource Technology Critical Overview of Biomass Feedstocks as Sustainable Substrates for the Production of Polyhydroxybutyrate (PHB). *Bioresour. Technol* **2020**, *311* (May), 123536.

(16) Koller, M. *Handbook of Polyhydroxyalkanoates*; CRC Press, 2020.

(17) Rivera-Briso, A. L.; Serrano-Aroca, Á. Poly(3-Hydroxybutyrate-Co-3-Hydroxyvalerate): Enhancement Strategies for Advanced Applications. *Polymers* **2018**, *10* (7), 732.

(18) Laycock, B.; Halley, P.; Pratt, S.; Werker, A.; Lant, P. The Chemomechanical Properties of Microbial Polyhydroxyalkanoates. *Prog. Polym. Sci* **2013**, *38* (3−4), 536−583.

(19) Owen, A. J.; Heinzel, J.; Škrbić, Ž.; Divjaković, V. Crystallization and Melting Behaviour of PHB and PHB/HV Copolymer. *Polymer* **1992**, *33* (7), 1563−1567.

(20) Tebaldi, M. L.; Maia, A. L. C.; Poletto, F.; de Andrade, F. V.; Soares, D. C. F. Poly(-3-hydroxybutyrate-co-3-hydroxyvalerate) (PHBV): Current advances in synthesis methodologies, antitumor applications and biocompatibility. *J. Drug Delivery Sci. Technol* **2019**, *51* (August2018), 115−126.
(21) You, J. W.; Chiu, H. J.; Shu, W. J.; Don, T. M. Influence of Hydroxyvalerate Content on the Crystallization Kinetics of Poly-(Hydroxybutyrate-Co-Hydroxyvalerate. *J. Polym. Res* **2003**, *10* (1), 47−54.
(22) Abbasi, M.; Pokhrel, D.; Coats, E. R.; Guho, N. M.; McDonald, A. G. Effect of 3-Hydroxyvalerate Content on Thermal, Mechanical, and Rheological Properties of Poly(3-Hydroxybutyrate-Co-3-Hydroxyvalerate) Biopolymers Produced from Fermented Dairy Manure. *Polymers* **2022**, *14* (19), 4140.
(23) Fosse, C.; Esposito, A.; Lemechko, P.; Salim, Y. S.; Causin, V.; Gaucher, V.; Bruzaud, S.; Sudesh, K.; Delbreilh, L.; Dargent, E. Effect of Chemical Composition on Molecular Mobility and Phase Coupling in Poly(3-Hydroxybutyrate-Co-3-Hydroxyvalerate) and Poly(3-Hydroxybutyrate-Co-3-Hydroxyhexanoate) with Different Comonomer Contents. *J. Polym. Environ* **2023**, *31* (10), 4430−4447.
(24) Carli, L. N.; Daitx, T. S.; Gonçalves, G. P. O.; Bianchi, O.; Crespo, J. S.; Mauler, R. S. Influence of the Thermomechanical Degradation on the Formation of the Crystalline Structure of PHBV Evaluated by Temperature-Resolved SAXS Experiments. *Polym. Eng. Sci* **2020**, *60* (11), 2945−2957.
(25) Xiang, H.; Wen, X.; Miu, X.; Li, Y.; Zhou, Z.; Zhu, M. Thermal Depolymerization Mechanisms of Poly(3-Hydroxybutyrate-Co-3-Hydroxyvalerate). *Prog. Nat. Sci.: mater. Int* **2016**, *26* (1), 58−64.
(26) Lee, C. H.; Sapuan, S. M.; Ilyas, R. A.; Lee, S. H.; Khalina, A. *Development and Processing of PLA, PHA, and Other Biopolymers*; Elsevier Inc., 2020.
(27) Renstad, R.; Karlsson, S.; Albertsson, A. Influence of Processing Induced Differences in Molecular Structure on the Biological and Non-Biological Degradation of Poly (3-Hydroxybutyrate-Co-3-Hydroxyvalerate), P(3-HB-Co-3-HV). *Polym. Degrad. Stab.* **1999**, *63*, 201−211.
(28) Shi, D.; Miao, Y.; Zhu, H.; Li, Y.; Wang, Z. Role of the Heat Treatment of Partial Melt Recrystallization Method on Microstructure Change and Toughness of Poly(3-Hydroxybutyrate-Co-3-Hydroxyvalerate) [P(HB-Co-HV)]. *Polymer* **2021**, *228* (May), 123874.
(29) Žiganova, M.; Merijs-Meri, R.; Zicāns, J.; Bochkov, I.; Ivanova, T.; Vīgants, A.; Ence, E.; Štrausa, E. Visco-Elastic and Thermal Properties of Microbiologically Synthesized Polyhydroxyalkanoate Plasticized with Triethyl Citrate. *Polymers* **2023**, *15* (13), 2896.
(30) Garcia-Garcia, D.; Quiles-Carrillo, L.; Balart, R.; Torres-Giner, S.; Arrieta, M. P. Innovative Solutions and Challenges to Increase the Use of Poly(3-Hydroxybutyrate) in Food Packaging and Disposables. *Eur. Polym. J* **2022**, *178* (August), 111505.
(31) Lyshtva, P.; Voronova, V.; Barbir, J.; Leal, W.; Kröger, S. D.; Witt, G.; Miksch, L.; Saborowski, R.; Gutow, L.; Frank, C.; Emmerstorfer-Augustin, A.; Agustin-Salazar, S. Degradation of a poly(3-hydroxybutyrate-co-3-hydroxyvalerate) (PHBV) compound in different environments. *Heliyon* **2024**, *10* (3), No. e24770.
(32) Meereboer, K. W.; Misra, M.; Mohanty, A. K. Review of Recent Advances in the Biodegradability of Polyhydroxyalkanoate (PHA) Bioplastics and Their Composites. *Green Chem* **2020**, *22* (17), 5519−5558.
(33) Bugnicourt, E.; Cinelli, P.; Lazzeri, A.; Alvarez, V. Polyhydroxyalkanoate (PHA): Review of Synthesis, Characteristics, Processing and Potential Applications in Packaging. *Express Polym. Lett* **2014**, *8* (11), 791−808.
(34) Helanto, K.; Matikainen, L.; Talj, R.; Rojas, O. J. Bio-Based Polymers for Sustainable Packaging and Biobarriers: A Critical Review. *BioResources* **2019**, *14* (2), 4902−4951.
(35) Masood, F. *Polyhydroxyalkanoates in the Food Packaging Industry*; Elsevier Inc., 2017.
(36) Tarrahi, R.; Fathi, Z.; SeydibeyoĞlu, M. Ö.; Doustkhah, E.; Khataee, A. Polyhydroxyalkanoates (PHA): From Production to Nanoarchitecture. *Int. J. Biol. Macromol* **2020**, *146*, 596−619.
(37) Park, H.; He, H.; Yan, X.; Liu, X.; Scrutton, N. S.; Chen, G. Q. PHA Is Not Just a Bioplastic! *Biotechnol. Adv* **2024**, *71* (January), 108320.
(38) Nanda, S.; Patra, B. R.; Patel, R.; Bakos, J.; Dalai, A. K. Innovations in Applications and Prospects of Bioplastics and Biopolymers: A Review. *Environ. Chem. Lett* **2022**, *20* (1), 379−395.
(39) Kumar, V.; Sehgal, R.; Gupta, R. Blends and Composites of Polyhydroxyalkanoates (PHAs) and Their Applications. *Eur. Polym. J* **2021**, *161* (August), 110824.
(40) Pandey, A.; Adama, N.; Adjallé, K.; Blais, J. F. Sustainable Applications of Polyhydroxyalkanoates in Various Fields: A Critical Review. *Int. J. Biol. Macromol* **2022**, *221* (September), 1184−1201.
(41) Shishatskaya, E. I.; Nikolaeva, E. D.; Vinogradova, O. N.; Volova, T. G. Experimental Wound Dressings of Degradable PHA for Skin Defect Repair. *J. Mater. Sci.: mater. Med* **2016**, *27* (11), 165.
(42) Ibrahim, M. I.; Alsafadi, D.; Alamry, K. A.; Hussein, M. A. Properties and Applications of Poly(3-Hydroxybutyrate-Co-3-Hydroxyvalerate) Biocomposites. *J. Polym. Environ* **2021**, *29* (4), 1010−1030.
(43) Khosravi-Darani, K.; Bucci, D. Z. Application of Poly-(Hydroxyalkanoate) in Food Packaging: Improvements by Nanotechnology. *Chem. Biochem. Eng. Q* **2015**, *29* (2), 275−285.
(44) Torres-Giner, S.; Figueroa-Lopez, K. J.; Melendez-Rodriguez, B.; Prieto, C.; Pardo-Figuerez, M.; Lagaron, J. M. Emerging Trends in Biopolymers for Food Packaging. *Sustainable Food Packaging Technology*; Wiley-VCH GmbH, 2021.
(45) Kalia, V. C.; Singh Patel, S. K.; Shanmugam, R.; Lee, J. K. Polyhydroxyalkanoates: Trends and Advances toward Biotechnological Applications. *Bioresour. Technol* **2021**, *326* (January), 124737.
(46) Emaimo, A. J.; Olkhov, A. A.; Iordanskii, A. L.; Vetcher, A. A. Polyhydroxyalkanoates Composites and Blends: Improved Properties and New Applications. *J. Compos. Sci* **2022**, *6* (7), 206.
(47) Kovalcik, A. Recent Advances in 3D Printing of Polyhydroxyalkanoates: A Review. *EuroBiotech J* **2021**, *5* (1), 48−55.
(48) Boey, J. Y.; Mohamad, L.; Khok, Y. S.; Tay, G. S.; Baidurah, S. A Review of the Applications and Biodegradation of Polyhydroxyalkanoates and Poly(Lactic Acid) and Its Composites. *Polymers* **2021**, *13* (10), 1544.
(49) Popa, M. S.; Frone, A. N.; Panaitescu, D. M. Polyhydroxybutyrate Blends: A Solution for Biodegradable Packaging? *Int. J. Biol. Macromol* **2022**, *207* (January), 263−277.
(50) Bairwan, R.; Yahya, E.; Gopakumar, D.; H.P.S, A. K. Recent Advances in Poly(3-Hydroxybutyrate-Co-3-Hydroxyvalerate) Biocomposites in Sustainable Packaging Applications. *Adv. Mater. Lett* **2024**, *15* (1), 2401−1739.
(51) Malmir, S.; Montero, B.; Rico, M.; Barral, L.; Bouza, R.; Farrag, Y. Effects of Poly (3-Hydroxybutyrate-Co-3-Hydroxyvalerate) Microparticles on Morphological, Mechanical, Thermal, and Barrier Properties in Thermoplastic Potato Starch Films. *Carbohydr. Polym* **2018**, *194* (April), 357−364.
(52) Romero-Castelán, E.; Rodríguez-Hernández, A. I.; Chavarría-Hernández, N.; López-Ortega, M. A.; López-Cuellar, M. D. R. Natural Antimicrobial Systems Protected by Complex Polyhydroxyalkanoate Matrices for Food Biopackaging Applications — A Review. *Int. J. Biol. Macromol* **2023**, *233* (January), 123418.
(53) Westlake, J. R.; Tran, M. W.; Jiang, Y.; Zhang, X.; Burrows, A. D.; Xie, M. Biodegradable Biopolymers for Active Packaging: Demand, Development and Directions. *Sustain. Food Technol* **2023**, *1* (1), 50−72.
(54) Gao, C.; Yu, L.; Liu, H.; Chen, L. Development of Self-Reinforced Polymer Composites. *Prog. Polym. Sci* **2012**, *37* (6), 767−780.
(55) Gil-Castell, O.; Badia, J. D.; Ingles-Mascaros, S.; Teruel-Juanes, R.; Serra, A.; Ribes-Greus, A. Polylactide-Based Self-Reinforced Composites Biodegradation: Individual and Combined Influence of

https://doi.org/10.1021/acsomega.4c05957
ACS Omega 2024, 9, 51073−51088

Temperature, Water and Compost. *Polym. Degrad. Stab* **2018**, *158*, 40−51.
(56) Zherebtsov, D.; Chukov, D.; Statnik, E.; Torokhov, V. Hybrid Self-Reinforced Composite Materials Based on Ultra-High Molecular Weight Polyethylene. *Materials* **2020**, *13* (7), 1739.
(57) Yadav, N.; Richter, T.; Löschke, O.; Abali, B. E.; Auhl, D.; Völlmecke, C. Towards Self-Reinforced PLA Composites for Fused Filament Fabrication. *Appl. Sci* **2023**, *13* (4), 2637.
(58) Wang, J.; Zhang, Q.; Cheng, Y.; Song, F.; Ding, Y.; Shao, M. Self-Reinforced Composites Based on Polypropylene Fiber and Graphene Nano-Platelets/Polypropylene Film. *Carbon* **2022**, *189*, 586−595.
(59) Le Gall, M.; Niu, Z.; Curto, M.; Catarino, A. I.; Demeyer, E.; Jiang, C.; Dhakal, H.; Everaert, G.; Davies, P. Behaviour of a Self-Reinforced Polylactic Acid (SRPLA) in Seawater. *Polym. Test* **2022**, *111* (April), 107619.
(60) Jurczyk, S.; Włodarczyk, J.; Kawalec, M.; Janeczek, H.; Michalak, M.; Sobota, M. The Bifunctionality of Poly[(R)-3-Hydroxybutyrate] in Self-Reinforced Composite Materials. *Polym. Test* **2017**, *63*, 614−620.
(61) Farrag, Y.; Ide, W.; Montero, B.; Rico, M.; Rodríguez-Llamazares, S.; Barral, L.; Bouza, R. Starch Films Loaded with Donut-Shaped Starch-Quercetin Microparticles: Characterization and Release Kinetics. *Int. J. Biol. Macromol* **2018**, *118*, 2201−2207.
(62) Liu, J.; Zhou, Z.; Li, H.; Yang, X.; Wang, Z.; Xiao, J.; Wei, D.-X.-X. Current Status and Challenges in the Application of Microbial PHA Particles. *Particuology* **2024**, *87*, 286−302.
(63) Barouti, G.; Jaffredo, C. G.; Guillaume, S. M. Advances in Drug Delivery Systems Based on Synthetic Poly(Hydroxybutyrate) (Co)-Polymers. *Prog. Polym. Sci* **2017**, *73*, 1−31.
(64) Rastogi, V. K.; Samyn, P. Synthesis of Polyhydroxybutyrate Particles with Micro-to-Nanosized Structures and Application as Protective Coating for Packaging Papers. *Nanomaterials* **2017**, *7* (1), 5.
(65) Rodríguez-Cendal, A. I.; Gómez-Seoane, I.; de Toro-Santos, F. J.; Fuentes-Boquete, I. M.; Señarís-Rodríguez, J.; Díaz-Prado, S. M. Biomedical Applications of the Biopolymer Poly(3-Hydroxybutyrate-Co-3-Hydroxyvalerate) (PHBV): Drug Encapsulation and Scaffold Fabrication. *Int. J. Mol. Sci* **2023**, *24* (14), 11674.
(66) Shegokar, R.; Nakach, M.Large-Scale Manufacturing of Nanoparticles—An Industrial Outlook. *Drug Delivery Aspects: Vol. 4: Expectations and Realities of Multifunctional Drug Delivery Systems*; Elsevier Inc., 2020; pp 57−77.
(67) Khairnar, S. V.; Pagare, P.; Thakre, A.; Nambiar, A. R.; Junnuthula, V.; Abraham, M. C.; Kolim, P.; Nyavanandi, D.; Dyawanapell, S. Review on the Scale-Up Methods for the Preparation of Solid Lipid Nanoparticles. *Pharmaceutics* **2022**, *14* (9), 1886.
(68) Muller, R. H.; Keck, C. M. Challenges and Solutions for the Delivery of Biotech Drugs - A Review of Drug Nanocrystal Technology and Lipid Nanoparticles. *J. Biotechnol* **2004**, *113* (1−3), 151−170.
(69) Parhi, R.; Suresh, P. Preparation and Characterization of Solid Lipid Nanoparticles-A Review. *Curr. Drug Discovery Technol* **2012**, *9* (1), 2−16.
(70) Hoogendijk, E.; Swider, E.; Staal, A. H. J.; White, P. B.; Van Riessen, N. K.; Glaßer, G.; Lieberwirth, I.; Musyanovych, A.; Serra, C. A.; Srinivas, M.; Koshkina, O. Continuous-Flow Production of Perfluorocarbon-Loaded Polymeric Nanoparticles: From the Bench to Clinic. *ACS Appl. Mater. Interfaces* **2020**, *12* (44), 49335−49345.
(71) Von Bomhard, S.; Schelhaas, K. P.; Alebrand, S.; Musyanovych, A.; Maskos, M.; Drese, K. S. Selective Solvent Evaporation from Binary Mixtures of Water and Tetrahydrofuran Using a Falling Film Microreactor. *Green Process. Synth* **2017**, *6* (4), 403−411.
(72) Kakkar, V.; Kaur, I. P. Preparation, Characterization and Scale-up of Sesamol Loaded Solid Lipid Nanoparticles. *Nanotechnol Dev* **2012**, *2* (1), No. e8.
(73) Bouza, R.; Del Mar Castro, M.; Dopico-García, S.; Victoria González-Rodríguez, M.; Barral, L. F.; Bittmann, B. Polylactic Acid and Poly(3-Hydroxybutyrate-Co-3-Hydroxyvalerate) Nano and Microparticles for Packaging Bioplastic Composites. *Polym. Bull* **2016**, *73* (12), 3485−3502.
(74) Koolman, J.; Roehm, K.-H. *Color Atlas of Biochemistry Second Edition, Revised and Enlarged*; Georg Thieme Verlag, 2005.
(75) Staff, R. H.; Landfester, K.; Crespy, D. Recent Advances in the Emulsion Solvent Evaporation Technique for the Preparation of Nanoparticles and Nanocapsules. *Adv. Polym. Sci* **2013**, *262* (October), 329−344.
(76) Leimann, F. V.; Filho, L. C.; Sayer, C.; Araújo, P. H. H. Poly(3-hydroxybutyrate-co-3- hydroxyvalerate) nanoparticles prepared by a miniemulsion/solvent evaporation technique: effect of phbv molar mass and concentration. *Braz. J. Chem. Eng* **2013**, *30* (2), 369−377.
(77) Antonietti, M.; Landfester, K. Polyreactions in Miniemulsions. *Prog. Polym. Sci* **2002**, *27* (4), 689−757.
(78) Samrot, A. V.; Samanvitha, S. K.; Shobana, N.; Renitta, E. R.; Kumar, P. S.; Kumar, S. S.; Abirami, S.; Dhiva, S.; Bavanilatha, M.; Prakash, P.; Saigeetha, S.; Shree, K. S.; Thirumurugan, R. The Synthesis, Characterization and Applications of Polyhydroxyalkanoates (Phas) and Pha-Based Nanoparticles. *Polymers* **2021**, *13* (19), 3302.
(79) Volant, C.; Balnois, E.; Vignaud, G.; Magueresse, A.; Bruzaud, S. Design of Polyhydroxyalkanoate (PHA) Microbeads with Tunable Functional Properties and High Biodegradability in Seawater. *J. Polym. Environ* **2022**, *30* (6), 2254−2269.
(80) Rao, J. P.; Geckeler, K. E. Polymer Nanoparticles: Preparation Techniques and Size-Control Parameters. *Prog. Polym. Sci* **2011**, *36* (7), 887−913.
(81) Crucho, C. I. C.; Barros, M. T. Polymeric Nanoparticles: A Study on the Preparation Variables and Characterization Methods. *Mater. Sci. Eng., C* **2017**, *80*, 771−784.
(82) bioplasticsnews.com. Frost & Sullivan Awards Bio-On for Best Cosmetic Innovation, 2018. https://bioplasticsnews.com/2018/10/08/frost-sullivan-awards-bio-best-cosmetic-innovation/.
(83) Choi, Y. H.; Park, J. J.; Sim, E. J.; Lee, E.; Yoon, K. C.; Park, W. H. Ecofriendly Poly(3-Hydroxybutyrate-Co-4-Hydroxybutyrate) Microbeads for Sanitary Products. *Int. J. Biol. Macromol* **2023**, *224* (October2022), 1487−1495.
(84) Wei, D. X.; Dao, J. W.; Chen, G. Q. A Micro-Ark for Cells: Highly Open Porous Polyhydroxyalkanoate Microspheres as Injectable Scaffolds for Tissue Regeneration. *Adv. Mater* **2018**, *30* (31), 1−10.
(85) Wei, D. X.; Dao, J. W.; Liu, H. W.; Chen, G. Q. Suspended Polyhydroxyalkanoate Microspheres as 3D Carriers for Mammalian Cell Growth. *Artif. Cells Nanomed. Biotechnol* **2018**, *46* (sup2), 473−483.
(86) Bini, R. A.; Silva, M. F.; Varanda, L. C.; da Silva, M. A.; Dreiss, C. A. Soft Nanocomposites of Gelatin and Poly(3-Hydroxybutyrate) Nanoparticles for Dual Drug Release. *Colloids Surf., B* **2017**, *157*, 191−198.
(87) Pettinelli, N.; Rodríguez-Llamazares, S.; Farrag, Y.; Bouza, R.; Barral, L.; Feijoo-Bandín, S.; Lago, F. Poly(Hydroxybutyrate-Co-Hydroxyvalerate) Microparticles Embedded in κ-Carrageenan/Locust Bean Gum Hydrogel as a Dual Drug Delivery Carrier. *Int. J. Biol. Macromol* **2020**, *146*, 110−118.
(88) Yang, S.; Miao, Q.; Huang, Y.; Jian, P.; Wang, X.; Tu, M. Preparation of Cinnamaldehyde-Loaded Polyhydroxyalkanoate/Chitosan Porous Microspheres with Adjustable Controlled-Release Property and Its Application in Fruit Preservation. *Food Packag. Shelf Life* **2020**, *26* (June), 100596.
(89) Bahrami, A.; Delshadi, R.; Assadpour, E.; Jafari, S. M.; Williams, L. Antimicrobial-Loaded Nanocarriers for Food Packaging Applications. *Adv. Colloid Interface Sci* **2020**, *278*, 102140.
(90) Malmir, S.; Montero, B.; Rico, M.; Barral, L.; Bouza, R.; Farrag, Y. Novel Self-Reinforced Films Based on Poly (3-Hydroxybutyrate-Co-3-Hydroxyvalerate) (PHBV) and PHBV Microparticles. *Polym. Eng. Sci* **2019**, *59*, No. E120−E128.
(91) Farrag, Y.; Montero, B.; Rico, M.; Barral, L.; Bouza, R. Preparation and Characterization of Nano and Micro Particles of Poly(3-Hydroxybutyrate-Co-3-Hydroxyvalerate) (PHBV) via Emulsi-

https://doi.org/10.1021/acsomega.4c05957
ACS Omega 2024, 9, 51073−51088

fication/Solvent Evaporation and Nanoprecipitation Techniques. *J. Nanoparticle Res* **2018**, *20* (3), 1−27.
(92) Scandola, M.; Focarete, M. L.; Adamus, G.; Sikorska, W.; Baranowska, I.; Świerczek, S.; Gnatowski, M.; Kowalczuk, M.; Jedliński, Z. Polymer Blends of Natural Poly(3-Hydroxybutyrate-Co-3-Hydroxyvalerate) and a Synthetic Atactic Poly(3-Hydroxybutyrate). Characterization and Biodegradation Studies. *Macromolecules* **1997**, *30* (9), 2568−2574.
(93) Senhorini, G. A.; Zawadzki, S. F.; Farago, P. V.; Zanin, S. M. W.; Marques, F. A. Microparticles of Poly(Hydroxybutyrate-Co-Hydroxyvalerate) Loaded with Andiroba Oil: Preparation and Characterization. *Mater. Sci. Eng., C* **2012**, *32* (5), 1121−1126.
(94) Zalloum, N. L.; Albino De Souza, G.; Martins, T. D. Single-Emulsion P(HB-HV) Microsphere Preparation Tuned by Copolymer Molar Mass and Additive Interaction. *ACS Omega* **2019**, *4* (5), 8122−8135.
(95) Barboza, F. M.; Machado, W. M.; Olchanheski Junior, L. R.; Padilha De Paula, J.; Zawadzki, S. F.; Fernandes, D.; Farago, P. V. PCL/PHBV Microparticles as Innovative Carriers for Oral Controlled Release of Manidipine Dihydrochloride. *Sci. World J* **2014**, *2014*, 268107.
(96) Hyuk Im, S.; Jeong, U.; Xia, Y. Polymer Hollow Particles with Controllable Holes in Their Surfaces. *Nat. Mater* **2005**, *4* (9), 671−675.
(97) Mahaling, B.; Katti, D. S. Fabrication of Micro-Structures of Poly [(R)-3-Hydroxybutyric Acid] by Electro-Spraying/-Spinning: Understanding the Influence of Polymer Concentration and Solvent Type. *J. Mater. Sci* **2014**, *49* (12), 4246−4260.
(98) Vadlja, D.; Koller, M.; Novak, M.; Braunegg, G.; Horvat, P. Footprint Area Analysis of Binary Imaged Cupriavidus Necator Cells to Study PHB Production at Balanced, Transient, and Limited Growth Conditions in a Cascade Process. *Appl. Microbiol. Biotechnol* **2016**, *100* (23), 10065−10080.
(99) Maia, J. L.; Santana, M. H. A.; Ré, M. I. The Effect of Some Processing Conditions on the Characteristics of Biodegradable Microspheres Obtained By an Emulsion Solvent Evaporation Process. *Braz. J. Chem. Eng* **2004**, *21* (1), 1−12.
(100) You, X.; Zhou, Y.; Jin, X.; Xiang, S.; Pei, X.; Zhou, H.; Liao, Z.; Tan, Y. Green Fabrication of PHBV Microbeads Using a Dimethyl Isosorbide Solvent for Skin Exfoliators. *Green Chemv* **2023**, *25* (23), 9948−9958.
(101) Koosha, F.; Muller, R. H.; Davis, S. S.; Davies, M. C. The Surface Chemical Structure of Poly(β-Hydroxybutyrate) Microparticles Produced by Solvent Evaporation Process. *J. Controlled Release* **1989**, *9* (2), 149−157.
(102) Requena, R.; Jiménez, A.; Vargas, M.; Chiralt, A. Effect of Plasticizers on Thermal and Physical Properties of Compression-Moulded Poly[(3-Hydroxybutyrate)-Co-(3-Hydroxyvalerate)] Films. *Polym. Test* **2016**, *56*, 45−53.
(103) da Costa, R. C.; Daitx, T. S.; Mauler, R. S.; da Silva, N. M.; Miotto, M.; Crespo, J. S.; Carli, L. N. Poly(Hydroxybutyrate-Co-Hydroxyvalerate)-Based Nanocomposites for Antimicrobial Active Food Packaging Containing Oregano Essential Oil. *Food Packaging And Shelf Life* **2020**, *26* (October), 2214−2894.
(104) Râpă, M.; Stefan, L. M.; Seciu-Grama, A.-M.; Gaspar-Pintiliescu, A.; Matei, E.; Zaharia, C.; Stănescu, P. O.; Predescu, C. Poly(3-Hydroxybutyrate-Co-3-Hydroxyvalerate) (P(3HB-Co-3HV))/Bacterial Cellulose (BC) Biocomposites for Potential Use in Biomedical Applications. *Polymers* **2022**, *14*, 5544.
(105) Zhu, H.; Lv, Y.; Shi, D.; Li, Y.; Wang, Z. Origin of the Double Melting Peaks of Poly(3-Hydroxybutyrate-Co-3-Hydroxyvalerate) with a High HV Content as Revealed by in Situ Synchrotron WAXD/SAXS Analyses. *J. Polym. Sci., Part B: polym. Phys* **2019**, *57* (21), 1453−1461.
(106) Rastogi, V. K.; Samyn, P. Novel Processing of Polyhydroxybutyrate with Micro-to Nanofibrillated Cellulose and Effect of Fiber Morphology on Crystallization Behaviour of Composites. *Express Polym. Lett* **2020**, *14* (2), 115−133.
(107) Gunaratne, L. M. W. K.; Shanks, R. A. Multiple Melting Behaviour of Poly(3-Hydroxybutyrate-Co-Hydroxyvalerate) Using Step-Scan DSC. *Eur. Polym. J* **2005**, *41* (12), 2980−2988.
(108) Cai, H.; Qiu, Z. Effect of Comonomer Content on the Crystallization Kinetics and Morphology of Biodegradable Poly(3-Hydroxybutyrate-Co-3-Hydroxyhexanoate). *Phys. Chem. Chem. Phys* **2009**, *11* (41), 9569−9577.
(109) Xu, P.; Wang, Q.; Yu, M.; Yang, W.; Weng, Y.; Dong, W.; Chen, M.; Wang, Y.; Ma, P. Enhanced Crystallization and Storage Stability of Mechanical Properties of Biosynthesized Poly (3-Hydroxybutyrate-Co-3-Hydroxyhexanate) Induced by Self-Nucleation. *Int. J. Biol. Macromol* **2021**, *184* (May), 797−803.
(110) Brandolt, S. D. F.; Daitx, T. S.; Mauler, R. S.; Ornaghi Junior, H. L.; Crespo, J. S.; Carli, L. N. Synergistic Effect between Different Clays and Plasticizer on the Properties of PHBV Nanocomposites. *Polym. Compos* **2019**, *40* (10), 3835−3843.
(111) Qiu, Y.; Fu, J.; Sun, B.; Ma, X. Sustainable Nanocomposite Films Based on SiO2and Biodegradable Poly(3-Hydroxybutyrate-Co-3-Hydroxyhexanoate) (PHBH) for Food Packaging. *E-Polym* **2021**, *21* (1), 072−081.
(112) Kopinke, F. D.; Remmler, M.; Mackenzie, K. Thermal Decomposition of Biodegradable Polyesters - I: Poly(β-Hydroxybutyric Acid). *Polym. Degrad. Stab* **1996**, *52* (1), 25−38.
(113) Öner, M.; Kirboga, S.; Abamor, E. Ş.; Karadaş, K.; Kral, Z. The Influence of Silicon-Doped Hydroxyapatite Nanoparticles on the Properties of Novel Bionanocomposites Based on Poly(3-Hydroxybutyrate-Co-3-Hydroxyvalerate). *Express Polym. Lett* **2023**, *17* (4), 417−433.
(114) Oberhoff, R. W. *Modifizierung Und Verarbeitung von Poly (3-Hydroxybuttersäure-Co-3-Hydroxyvaleriansäure) (PHBV) Mit Kugelförmigen Mikropartikeln*; Technischen Universität Dresden, 2005.
(115) Mysiukiewicz, O.; Barczewski, M.; Skórczewska, K.; Matykiewicz, D. Correlation between Processing Parameters and Degradation of Different Polylactide Grades during Twin-Screw Extrusion. *Polymers* **2020**, *12* (6), 1333.
(116) Vanheusden, C.; Samyn, P.; Goderis, B.; Hamid, M.; Reddy, N.; Ethirajan, A.; Peeters, R.; Buntinx, M. Extrusion and Injection Molding of Poly(3-Hydroxybutyrate-Co-3-Hydroxyhexanoate) (Phbhhx): Influence of Processing Conditions on Mechanical Properties and Microstructure. *Polymers* **2021**, *13* (22), 4012.
(117) Mazur, K.; Singh, R.; Friedrich, R. P.; Genç, H.; Unterweger, H.; Sałasińska, K.; Bogucki, R.; Kuciel, S.; Cicha, I. The Effect of Antibacterial Particle Incorporation on the Mechanical Properties, Biodegradability, and Biocompatibility of PLA and PHBV Composites. *Macromol. Mater. Eng* **2020**, *305* (9), 1−15.
(118) Najah, M. I.; Aisyah, R.; Adzila, S.; Haq, R. H. A. Mechanical Properties of Calcium Phosphate Reinforced Polyhydroxyalkanoate (PHA) Biocomposite. *J. Thermoplast. Compos. Mater* **2023**, *36* (8), 3294−3311.
(119) Tamiya, T.; Hsu, Y. I.; Asoh, T. A.; Uyama, H. Improvement of Interfacial Adhesion between Poly(3-Hydroxybutyrate-Co-3-Hydroxyhexanoate) and Silica Particles. *Ind. Eng. Chem. Res* **2020**, *59* (30), 13595−13602.
(120) Bossu, J.; Le Moigne, N.; Dieudonné-George, P.; Dumazert, L.; Guillard, V.; Angellier-Coussy, H. Impact of the Processing Temperature on the Crystallization Behavior and Mechanical Properties of Poly[R-3-Hydroxybutyrate-Co-(R-3-Hydroxyvalerate)]. *Polymer* **2021**, *229* (June), 123987.
(121) Kostic, D.; Vukasinovic-Sekulic, M.; Armentano, I.; Torre, L.; Obradovic, B. Multifunctional Ternary Composite Films Based on PLA and Ag/Alginate Microbeads: Physical Characterization and Silver Release Kinetics. *Mater. Sci. Eng* **2019**, *98* (January), 1159−1168.
(122) Ward, I. M.; Sweeney, I. M. *Mechanical Properties of Solid Polymers*, 3rd ed.; Wiley, 2013; Vol. 3.
(123) Manikandan, N. A.; Pakshirajan, K.; Pugazhenthi, G. Preparation and Characterization of Environmentally Safe and Highly Biodegradable Microbial Polyhydroxybutyrate (PHB) Based Gra-

https://doi.org/10.1021/acsomega.4c05957
ACS Omega 2024, 9, 51073−51088

phene Nanocomposites for Potential Food Packaging Applications. *Int. J. Biol. Macromol* **2020**, *154*, 866−877.
(124) Qasim, U.; Fatima, R.; Usman, M. Efficient Barrier Properties of Mechanically Enhanced Agro-Extracted Cellulosic Biocomposites. *Mater. Today Chem* **2020**, *18*, 100378.
(125) Zhang, J.; Cran, M. J. Production of Polyhydroxyalkanoate Nanoparticles Using a Green Solvent. *J. Appl. Polym. Sci* **2022**, *139* (23), 1−9.

https://doi.org/10.1021/acsomega.4c05957
ACS Omega 2024, 9, 51073−51088